Direct Kinematics Solution of 3-RCC Parallel Robot using a Semi-Analytical Homotopy Method

Seyed Mojtaba Varedi-Koulaei*
Department of Mechanical and Mechatronics Engineering,
Shahrood University of Technology, Iran
E-mail: varedi@shahroodut.ac.ir
*Corresponding author

Masoumeh Rahimi
Department of Mechanical Engineering, Faculty of Engineering,
Golestan University, Iran
E-mail: m.rahimi@gu.ac.ir

Received: 7 March 2018, Revised: 23 June 2018, Accepted: 27 July 2018

Abstract: Parallel robots are closed-loop mechanisms presenting very good performances in terms of accuracy, rigidity, and the ability to manipulate large loads. Inverse kinematics problem for most parallel robots is straightforward, while the direct kinematics is not. The latter requires the solution of the system of nonlinear coupled algebraic equations and has many solutions. Except in a limited number of these problems, there is difficulty in finding exact analytical solutions. So these nonlinear simultaneous equations should be solved using some other methods. Continuation or path-following methods are standard numerical techniques to trace the solution paths defined by the Homotopy. This paper presents the direct kinematics solutions for a 3RCC parallel robot by using a semi-analytical Homotopy method called Homotopy Continuation Method (HCM). The HCM has some advantages over the conventional methods and alleviates drawbacks of the traditional numerical techniques, namely; the acquirement of good initial guess values, the problem of convergence and computing time. The direct kinematic problem of the 3RCC parallel robot leads to a system of nonlinear equations with 9 equations and 9 unknown parameters. The proposed method solved these nonlinear equations and extracted all the 36 solutions. Results indicate that this method is effective and reduces computation time in comparison with the Newton–Raphson method.

Keywords: Direct Kinematics, Homotopy Continuation Method, Nonlinear Equations, Numerical Methods, Parallel Manipulator

Reference: Varedi Koulaei, S.M., Rahimi, M., "Direct Kinematics Solution of the 3-RCC Parallel Robot Using a Semi-Analytical Homotopy Method", Int J of Advanced Design and Manufacturing Technology, Vol. 12/No. 1, 2019, pp. 1–12.

Biographical notes: Seyed Mojtaba Varedi-Koulaei received his PhD in Mechanical Engineering from Babol Noshirvani University of Technology, in 2015. He is currently Assistant Professor at the Department of Mechanical Engineering, Shahrood University of Technology, Shahrood, Iran. His current research interest includes Robotics, Mechanism Design, and Optimization. **Masoumeh Rahimi** received his PhD in Mechanical Engineering from Babol Noshirvani University of Technology, in 2015. He is currently Assistant Professor at the Department of Mechanical Engineering, Golestan University, Gorgan, Iran.

1 INTRODUCTION

Parallel manipulators are closed-loop mechanisms presenting very good performances in terms of accuracy, rigidity and ability to manipulate large loads. They have been used in a large number of applications ranging from astronomy to flight simulators, and are becoming increasingly popular in the machine-tool industry. They typically consist of two platforms, which are connected by several extendable limbs or legs. The early design of the parallel manipulator was a six-linear jack system devised as a tire-testing machine proposed by Gough and Whitehall [1]. Then, Stewart [2] designed a general six-legged platform manipulator as an airplane simulator. After that, Hunt [3] suggested the use of the Stewart platform mechanism as a robot manipulator. Since then, parallel mechanisms had been studied extensively [4-11]. The direct kinematics of serial manipulators is straightforward while their inverse kinematics is quite complicated requiring the solution of a system of nonlinear equations. In contrast, the inverse kinematics of parallel manipulators is relatively straightforward, while its direct kinematics is challenging [12]. It involves the solution of a system of nonlinear coupled algebraic equations in the variables describing the platform posture and has many solutions [13]. Except in a limited number of these problems, there is some difficulty in finding exact analytical solutions. So these nonlinear simultaneous equations should be solved using some other methods.

In recent decades, numerical calculation methods were used to help us. As the numerical methods developed, semi-exact analytical counterpart also extended. Most scientists believe that a combination of numerical and semi-exact analytical methods can also result in useful achievements [14-16]. In the process of solving a kinematics problem of a robot, some troublesome simultaneous non-linear equations may be generated. Today, there are many different methods developed to deal with such non-linear equations, including the Newton–Raphson method [17-18] which is very efficient in the convergence speed. In addition to the selected method, the initial value significantly affects the convergence. An intelligently selected initial guess value may lead to a quick equation solution; while, a deviated initial guess usually causes divergence. Homotopy continuation method is a type of perturbation method [17-18]. It can guarantee the solution by a certain path, if the auxiliary homotopy function is well selected. It does not share the drawbacks of the traditional numerical techniques, namely; the acquirement of good initial guess values, the problem of convergence and computational time. This method, known as early as the 1930s, was used by a kinematician in the 1960s for solving the mechanism synthesis problems. The latest development was done by Morgan [19], Garcia [20] and Allgower [21]. Also, Wu [17-18] presented some techniques by combining Newton's and homotopy methods to avoid divergence in solving nonlinear equations.

This paper presents the direct kinematics solutions for a 3RCC parallel robot by using a semi-analytical Homotopy method called Homotopy Continuation Method (HCM). The HCM has some advantages over the conventional methods and alleviates drawbacks of the traditional numerical techniques, namely; the acquirement of good initial guess values, the problem of convergence and computing time. One of the best aspects of the proposed method is that it can extract all the solutions of the equations. This feature is very useful especially in the solution of the direct kinematics problem of a robot.

2 THE HOMOTOPY CONTINUATION METHOD (HCM)

When dealing with any numerical problem, e.g., the Newton–Raphson method, there are two troublesome questions. One is that proper initial guesses are not easy to introduce and the other is related to whether the implemented method will converge to meaningful solutions or not. The homotopy continuation method (HCM) can eliminate these shortcomings [17]. This method has been used by many researchers in the past decades [22-24]. HCM provides a useful approach to find the zeros of a system of nonlinear equations in a globally convergent way. HCM belongs to the family of continuation methods and similar to all these methods, they represent a way to find a solution of a problem by constructing a new problem, simpler than the original one, and then gradually deforming this simpler problem into the original one keeping track of the series of zeros that connect the solution of the simpler problem to that of the original, harder one. The greatest advantage of the HCM is that, under some conditions, they offer a way to have a globally convergent method to find the zeros of any function $f: R^n \rightarrow R^n$.

In this method, the homotopy continuation functions are written with auxiliary homotopy function firstly and then this system of nonlinear equations by the Newton-Raphson method is solved.

Let us consider the following system of nonlinear equations:

$$\mathrm{F(X)} = 0 \quad \text{i.e} \begin{cases} \mathrm{f(x, y, \dots, z)} = 0, \\ \mathrm{g(x, y, \dots, z)} = 0, \\ \quad\quad . \\ \quad\quad . \\ \quad\quad . \\ \mathrm{h(x, y, \dots, z)} = 0, \end{cases} \tag{1}$$

The numerical iteration formula of Newton's method for solving the system of these equations is given as:

$$\begin{bmatrix} \frac{\partial f(x_n, y_n, \dots)}{\partial x} & \frac{\partial f(x_n, y_n, \dots)}{\partial y} & . & . & . \\ \frac{\partial g(x_n, y_n, \dots)}{\partial x} & \frac{\partial g(x_n, y_n, \dots)}{\partial y} & . & . & . \\ . & . & . & & \\ . & . & & . & \\ . & . & & & . \end{bmatrix} \begin{bmatrix} x_{n+1} - x_n \\ y_{n+1} - y_n \\ . \\ . \\ . \end{bmatrix} = \begin{bmatrix} -f(x_n, y_n, \dots) \\ -g(x_n, y_n, \dots) \\ . \\ . \\ . \end{bmatrix} \tag{2}$$

Given a system of equations in n variables $x_1, x_2, \dots, x_n$ equations are modified by omitting some of the terms and adding new ones until a new system of equations are formed, the solutions to which may be easily guessed/given/known. Then in order to reach the solution, the coefficients of the new system into the coefficients of the original system are deformed by a series of small increments. This is called the homotopy continuation technique. In order to find the solutions of the "Eqs. (1)", a new simple start system or call auxiliary homotopy function [17], [22] is chosen, as:

$$G(X) = 0 \tag{3}$$

$G(X)$ must be known or controllable and easy to solve. Then, the homotopy continuation function can be written as follows:

$$H(X, t) \equiv t\,F(X) + (1 - t)G(X) = 0 \tag{4}$$

Where t is an arbitrary parameter which varies from 0 to 1, i.e. $t \in [0, 1]$. Therefore, the following two boundary conditions [20], [26] are:

$$\begin{aligned} H(X, 0) &= G(X) \\ H(X, 1) &= F(X) \end{aligned} \tag{5}$$

Our goal is to solve the $H(X, t) = 0$ instead of $F(X) = 0$ by varying the parameter t from 0 to 1 to avoid divergence. Hence the "Eq. (2)" is rewritten as [17]:

$$\begin{bmatrix} \frac{\partial H_1(x_n, y_n, \dots)}{\partial x} & \frac{\partial H_1(x_n, y_n, \dots)}{\partial y} & . & . & . \\ \frac{\partial H_2(x_n, y_n, \dots)}{\partial x} & \frac{\partial H_2(x_n, y_n, \dots)}{\partial y} & . & . & . \\ . & . & . & & \\ . & . & & . & \\ . & . & & & . \end{bmatrix} \begin{bmatrix} x_{n+1} - x_n \\ y_{n+1} - y_n \\ . \\ . \\ . \end{bmatrix} = \begin{bmatrix} -H_1(x_n, y_n, \dots) \\ -H_2(x_n, y_n, \dots) \\ . \\ . \\ . \end{bmatrix} \tag{6}$$

To avoid divergence, Wu [17] provided some useful choices about the auxiliary homotopy function which can be summarized as a polynomial, harmonic, exponential or any combinations of them. By appropriate choosing/adjusting the auxiliary homotopy function, the solutions of the cited "Eq. (1)" becomes available [18].

3 KINEMATICS MODEL OF 3-RCC PARALLEL ROBOT

This paper presents a novel parallel mechanism, which only gives pure three-translation output by which the direct position analysis is addressed. Moreover, as far as numerical solutions for the forward kinematics of the parallel mechanism with specific given dimensions are demonstrated, these analyses provide a solid foundation for kinematics of this novel parallel robot mechanism [25]. "Fig. 1" illustrates the structure of the parallel manipulator with pure three-translation discussed in this paper. It consists of the upper moving platform 1, lower fixed frame 2 and three connecting SOC (a set of the serial binary link) limbs. Every limb has one revolute joint and two cylindrical joints. Link 4 connected to the fixed lower frame 2 by using revolute joints A_0 (B_0 and C_0) is connected with link 3 by using cylindrical joints A_1(B_1, C_1), while link 3 is connected to the upper moving platform 1 by using cylindrical joints A_2 (B_2 and C_2). In general, the axle of the revolute joints A_0, B_0 and C_0 can be perpendicular to each other as in "Fig. 1" or not, while the axle of joint A_1 is perpendicular to that of joint A_2 but parallel to that of joint A_0, i.e. $(3 - R \parallel C \perp C)$ type (here, R means revolute joint, C means cylindrical joint). Therefore, the motion of the three motors A_0, B_0 and C_0 in the lower fixed frame 2 will control the position of the upper moving platform 2, which are translations along the x, y and z-axes without any rotations. If cutting tools are installed in the upper moving platform, this mechanism can be used as virtual CNC machine based on parallel mechanism. If measurement equipment is installed in the upper moving platform, it can be used as a coordinate measurement machine (CMM) based on parallel mechanism [25].

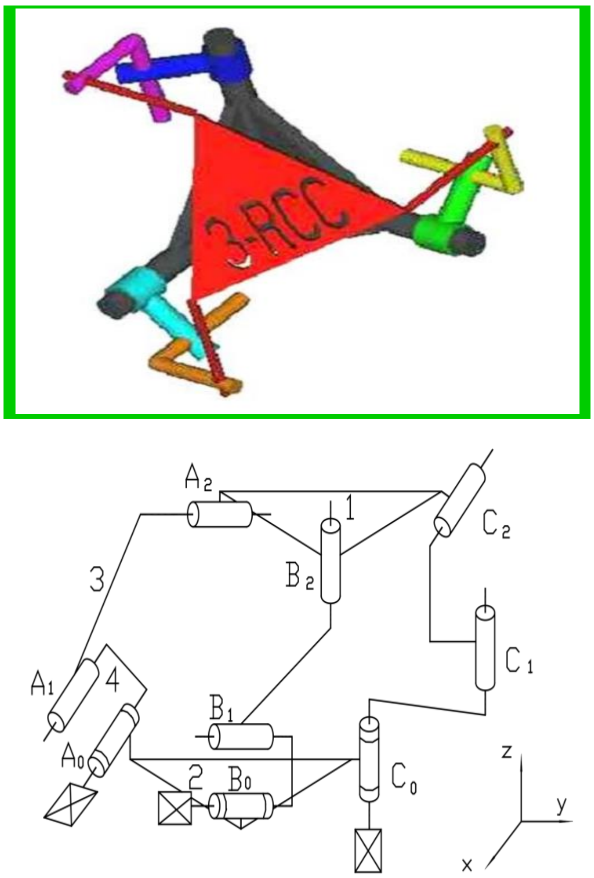

Fig. 1 Configuration of a novel parallel mechanism (3RCC) with pure three-translation [25].

For simplicity, a right-hand coordinate system $O-xyz$ is used for displacement analysis of the parallel mechanism shown in "Fig. 2", whose the x-axis is coincident with the axis of A_0 revolute joint, the y-axis is coincident with the axis of B_0 revolute joint and z-axis is coincident with the axis of C_0 revolute joint [25].
In "Fig. 2", the notations are [25]:

- α is the angle between the positive y-axis and vector A_0A_1, β is the angle between positive z-axis and vector B_0B_1 and γ is the angle between the positive x-axis and vector C_0C_1.
- θ_{11} is the rotation angle of the cylindrical joint A_1 around x_1-axis.
- θ_{21} is the rotation angle of the cylindrical joint B_1 around the y_2-axis.
- θ_{31} is the rotation angle of the cylindrical joint C_1 around the z_3-axis.
- l, m, n are the link lengths of the link A_0A_1, B_0B_1 and C_0C_1.

The signs of all angles above are determined by the right-hand rule. Coordinates of A_0, B_0, C_0 are $(a_0, 0, 0)$, $(0, b_0, 0)$, and $(0, 0, c_0)$. Vector lengths are shown in "Fig. 2" proportionally, where, three local coordinate systems, $A_2 - x_1y_1z_1$, $B_2 - x_2y_2z_2$, and $C_2 - x_3y_3z_3$ are established with their origin at points A_2, B_2 and C_2 respectively. Because of the perpendicular relations among the joints of every limb, x_1, y_2, z_3 are respectively coincident with the axis of cylindrical joints A_1, B_1 and C_1. Thus, it can be easily observed from "Fig. 2" that a, b and c are three input motions of joint A_0, B_0 and C_0. Intermediate cylindrical joints A_1, B_1 and C_1 can be transformed into A_2, B_2 and C_2 via translations s_{11}, s_{21}, s_{31} and rotations θ_{11}, θ_{21}, θ_{31}. And, cylindrical joints A_2, B_2 and C_2, which connects the three limbs to the upper moving frame, can be transformed to the points A_3, B_3 and C_3 via translations s_{21}, s_{22}, s_{32} without any rotations [25].

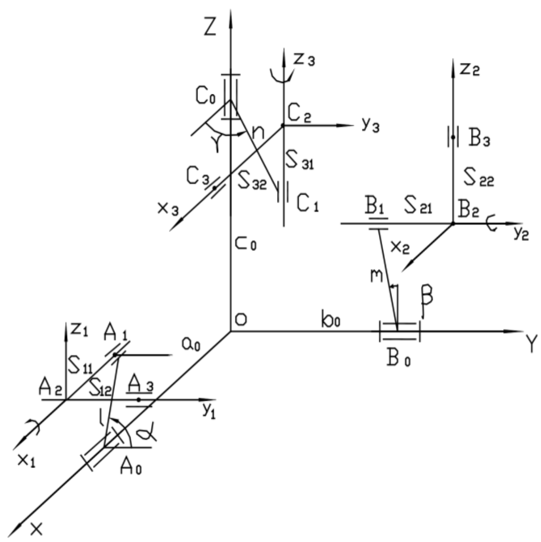

Fig. 2 The coordinate system of displacement analysis [25].

3.1. Coordinates of A_3, B_3, and C_3

Based on "Fig. 2", the coordinates of the point A_3, B_3, C_3 can be expressed as below by using D–H transformations [25]:

$$\begin{bmatrix} X_{A_3} \\ Y_{A_3} \\ Z_{A_3} \end{bmatrix} = \begin{bmatrix} a_0 + s_{11} \\ l\ cos\alpha + s_{12}\ cos\theta_{11} \\ l\ sin\alpha + s_{12}\ sin\theta_{11} \end{bmatrix} \quad (7)$$

$$\begin{bmatrix} X_{B_3} \\ Y_{B_3} \\ Z_{B_3} \end{bmatrix} = \begin{bmatrix} m\ sin\beta + s_{22}\ cos\theta_{21} \\ b_0 +\ s_{21} \\ m\ cos\beta + s_{22}\ sin\theta_{21} \end{bmatrix} \tag{8}$$

$$\begin{bmatrix} X_{C_3} \\ Y_{C_3} \\ Z_{C_3} \end{bmatrix} = \begin{bmatrix} n\ sin\gamma + s_{32}\ cos\theta_{31} \\ n\ sin\gamma + s_{32}\ sin\theta_{31} \\ c_0 +\ s_{31} \end{bmatrix} \tag{9}$$

3.2. Orientation of the Axis of Cylindrical Joints A3, B3, C3

Vector representation of the orientation of the axis of cylindrical joints A_3, B_3 and C_3 in the moving platform can be represented as [25]:

$$\begin{aligned}\overrightarrow{A_3} &= [i, j, k] \\ &= [X_{A_3} - X_{A_2}, Y_{A_3} - Y_{A_2}, Z_{A_3} - Z_{A_2}]^T \\ &= [0, s_{12}\ cos\theta_{11}, s_{12}\ sin\theta_{11}]^T\end{aligned} \tag{10}$$

$$\begin{aligned}\overrightarrow{B_3} &= [u, v, w] \\ &= [X_{B_3} - X_{B_2}, Y_{B_3} - Y_{B_2}, Z_{B_3} - Z_{B_2}]^T \\ &= [s_{22}\ cos\theta_{21}, 0, s_{22}\ sin\theta_{21}]^T\end{aligned} \tag{11}$$

$$\begin{aligned}\overrightarrow{C_3} &= [r, s, t] \\ &= [X_{C_3} - X_{C_2}, Y_{C_3} - Y_{C_2}, Z_{C_3} - Z_{C_2}]^T \\ &= [s_{32}\ cos\theta_{31}, s_{32}\ sin\theta_{31}, 0]^T\end{aligned} \tag{12}$$

3.3. Establishment of Displacement Constraint Equations

The displacement differences between the coordinates of points A_3, B_3 and C_3 along the x, y and z-axes must be constant, since the moving platform 1 has only three translations without any rotation. Therefore, there are six independent equations as follows [25]:

$$X_{A_3} - X_{B_3} = a_0 + s_{11} - m\ sin\beta - s_{22}\ cos\theta_{21} = M_1 \tag{13}$$

$$Y_{A_3} - Y_{B_3} = l\ cos\alpha + s_{12}\ cos\theta_{11} - m\ cos\beta - s_{22}\ sin\theta_{21} = P_1 \tag{14}$$

$$Z_{A_3} - Z_{B_3} = l\ sin\alpha + s_{12}\ sin\theta_{11} - m\ cos\beta - s_{22}\ sin\theta_{21} = P_1 \tag{15}$$

$$X_{A_3} - X_{C_3} = a_0 + s_{11} - n\ cos\gamma - s_{32}\ cos\theta_{31} = M_2 \tag{16}$$

$$Y_{A_3} - Y_{C_3} = l\ cos\alpha + s_{12}\ cos\theta_{11} - n\ sin\gamma - s_{32}\ sin\theta_{31} = N_2 \tag{17}$$

$$Z_{A_3} - Z_{C_3} = l\ sin\alpha + s_{12}\ sin\theta_{11} - c_0 - s_{31} = P_2 \tag{18}$$

Where $M_i, N_i, P_i\ (i = 1, 2)$ are known, which can be calculated from the initial assemblage configuration of the mechanism while Eqs. (13)– (15) are used for points between A_3 and B_3, and "Eqs. (16)– (18)" are employed for points between A_3 and C_3.

Because of the axis of revolute joints A_0, B_0, C_0 are perpendicular to each other and the one revolute joint and two cylindrical joints in each limb satisfy the relationship like R ∥ C ⊥ C, the axes at cylindrical joint A_3, B_3 and C_3 are also perpendicular to each other. That is, the vectors in "Eqs. (10)– (12)" are perpendicular to each other that are [25]:

$$i \cdot u + j \cdot v + k \cdot w = s_{12}\ sin\theta_{11} \cdot s_{22}\ cos\theta_{21} = 0 \tag{19}$$

$$u \cdot r + v \cdot s + w \cdot t = s_{22}\ cos\theta_{21} \cdot s_{32}\ cos\theta_{31} = 0 \tag{20}$$

$$i \cdot r + j \cdot s + k \cdot t = s_{12}\ cos\theta_{11} \cdot s_{32}\ sin\theta_{31} = 0 \tag{21}$$

4 DIRECT KINEMATICS

Solving the direct kinematics of the manipulator involves finding the location (position and orientation) of the moving platform, given joint variables (Given input angles α,β and γ are known). Nine unknown variables $((s_{11}, s_{21}, s_{31}), (\theta_{11}, \theta_{21}, \theta_{31}), (s_{12}, s_{22}, s_{32}))$ of the system of nonlinear equations can be solved by using the homotopy continuation method. The homotopy continuation functions (equation 4) for this system of equations are as follows:

$$H_1 = (a_0 + s_{11} - m\sin(\beta) - s_{22}\cos(\theta_{21}) - M_1) \times t + (1 - t) \times G_1 \tag{22a}$$

$$H_2 = (l\cos(\alpha) + s_{12}\cos(\theta_{11}) - b_0 - s_{21} - N_1) \times t + (1 - t) \times G_2 \tag{22b}$$

$$H_3 = (l\sin(\alpha) + s_{12}\sin(\theta_{11}) - m\cos(\beta) - s_{22}\sin(\theta_{22}) - p_1) \times t + (1 - t) \times G_3 \tag{22c}$$

$$H_4 = (a_0 + s_{11} - n\cos(\gamma) - s_{32}\cos(\theta_{31}) - M_2) \times t + (1 - t) \times G_4 \tag{22d}$$

$$H_5 = (l\cos(\alpha) + s_{12}\cos(\theta_{11}) - n\sin(\gamma) - s_{32}\sin(\theta_{31}) - N_1) \times t + (1 - t) \times G_5 \tag{22e}$$

$$H_6 = (l\sin(\alpha) + s_{12}\sin(\theta_{11}) - c_0 - s_{31} - p_2) \times t + (1 - t) \times G_6 \tag{22f}$$

$$H_7 = (s_{12}\sin(\theta_{11}) \times s_{12}\cos(\theta_{21})) \times t + (1 - t) \times G_7 \tag{22g}$$

$$H_8 = (s_{22}\cos(\theta_{21}) \times s_{32}\cos(\theta_{31})) \times t + (1 - t) \times G_8 \tag{22h}$$

$$H_9 = (s_{12}\cos(\theta_{11}) \times s_{32}\cos(\theta_{31})) \times t + (1 - t) \times G_9 \quad (22i)$$

In order to obtain the results of these equations, the geometric parameters of the manipulator are determined using the following assumptions:

$$\begin{aligned} &a_0 = b_0 = c_0 = 80, \\ &l = m = n = 30, \\ &M_1 = N_1 = P_1 = M_2 = N_2 = P_2 = 30; \\ &\alpha = \beta = \gamma = \pi/5 \end{aligned} \quad (23)$$

The homotopy parameter t varies from 0 to 1 ($\Delta t = 0.0001$) and initial guesses of unknown parameters are: $(s_{11}, s_{21}, s_{31}, s_{12}, s_{22}, s_{32}, \theta_{11}, \theta_{21}, \theta_{31}) = (1, 1, 1, 1, 1, 1, 1, 1, 1)$ (in radians). Because this method is not sensitive to the initial guesses, the simplest value is chosen for these parameters.

The Eqs. (22a)– (22i) are solved by using the Newton–Raphson method for which the auxiliary homotopy functions ($G_i, i = 1, \dots, 9$) change. The auxiliary homotopy functions are given in the Appendix. By changing these functions, different solutions are extracted. It is worth noting that, a different auxiliary function can lead to the same results, thus another choice for these functions must be considered. Tables in Appendix show that auxiliary homotopy functions are very simple and famous functions. Moreover, changing the initial guesses of the unknown parameters does not have a significant effect on the result. In Table 1, the 36 real solutions of these nonlinear equations are shown.

Table 1 36 solutions for the system of equations

Sols.	S11	S21	S31	S12	S22	S32	θ11	θ21	θ31
1	-32.3668	-62.3662	-92.3664	23.3627	36.6360	6.6377	0	-1.5708	-3.1416
2	-32.3658	-62.3654	-92.3664	23.3634	-36.6360	6.6368	0	133.5177	-15.708
3	-32.3668	-62.3667	-92.3664	23.3634	36.6360	-6.6377	-351.858	-1.5708	0
4	-32.3668	-62.3674	-92.3664	-23.3627	36.6360	6.6377	-298.451	-7.584	442.9646
5	-32.3661	-62.3667	-92.3664	-23.3634	-36.6379	6.6371	47.1239	1.5708	-9.4248
6	-32.3661	-62.3662	-92.3665	-23.3627	36.6360	-6.6362	15.708	-70.6858	0
7	-32.3668	-62.3655	-92.3665	23.3634	-36.6379	-6.6370	0	1.5708	0
8	-32.3668	-62.3655	-92.3665	-23.3634	-36.6360	-6.6368	40.8407	-92.677	-12.5664
9	-25.7297	-62.3662	-92.3664	23.3627	37.2341	0	0	-1.3916	0
10	-25.7297	-62.3667	-92.3664	23.3634	-37.2341	0	12.5664	-23.3827	2.9497
11	-25.7297	-62.3667	-92.3664	-23.3634	37.2339	0	-3.1416	-1.3916	-0.2739
12	-25.7297	-62.3667	-92.3664	-23.3634	-37.2341	0	0	-1.3916	0
13	-32.3668	-85.7286	-92.3662	0	36.6360	24.2872	0	-1.5708	17.002
14	-32.3668	-85.7286	-92.3662	0	-36.6360	24.2879	0	83.2522	-1.8476
15	-32.3668	-85.7286	-92.3667	0	36.6360	-24.2879	0	-629.889	1.2940
16	-32.3668	-85.7286	-92.3667	0	-36.6360	-24.2879	0	-17.2788	1.2940
17	-32.3668	-85.7286	-55.7298	36.6364	0	24.2874	447.677	1.5708	-165.21
18	-32.3667	-85.7303	-55.7298	36.6364	0	-24.2878	39.2699	29.8451	-11.2724
19	-32.3661	-85.7303	-55.7292	-36.6375	0	24.2873	-1.5708	1.5708	-1.8476
20	32.3668	-85.7303	-55.7298	-36.6364	0	-24.2874	-64.4026	-7.8540	-42.6883
21	-32.3668	-62.3671	-55.7300	43.4518	0	6.6364	-281.74	-1.5708	185.354
22	-32.3668	-62.3671	-55.7300	-43.4518	0	6.6318	-303.731	133.5177	235.6194
23	-32.3661	-62.3658	-55.7301	43.4518	0	-6.6375	13.5695	39.9467	0
24	-32.3668	-62.3658	-55.7301	-43.4518	0	-6.6364	-2.1385	-1.5708	0
25	-25.7286	-62.3659	-55.7300	43.4517	6.6376	0	-80.6783	-508.938	-78.7039
26	-25.7304	-62.3659	-55.7300	-43.4517	6.6358	0	-8.4217	559.2035	24.3473
27	-25.7299	-62.3700	-55.7890	43.4528	-6.6368	0	1.0030	116.2389	53.2833
28	-25.7304	-62.3658	-55.7300	-43.4518	-6.6358	0	-14.7048	-53.4071	-65.1880
29	-25.7291	-85.7286	-55.7298	36.6364	6.6371	23.3630	1.5708	0	-1.5708
30	-25.7299	-85.7286	-55.7298	-36.6364	6.6363	23.3630	-1.5708	0	-1.5708
31	-25.7291	-85.7286	-55.7298	36.6364	-6.6371	23.3631	1.5708	-3.1416	-1.5708
32	-25.7291	-85.7286	-55.7303	36.6364	6.6371	-23.3630	1.5708	0	1.5708
33	-25.7291	-85.7286	-55.7303	36.6364	-6.6371	-23.3631	1.5708	-3.1416	1.5708
34	-25.7299	-85.7286	-55.7298	-36.6364	-6.6363	23.3631	-1.5708	-3.1416	-1.5708
35	-25.7299	-85.7286	-55.7303	-36.6364	6.6363	-23.3630	-1.5708	0	1.5708
36	-25.7299	-85.7286	-55.7303	-36.6364	-6.6363	-23.3631	-1.5708	-3.1416	1.5708

By substituting the nine previous intermediate variables into "Eqs. (7)– (9)", the coordinates of points A_3, B_3 and C_3 as well as the coordinates of any given point in the moving platform can be calculated. Supposing the gravity point of the triangle formed by points A_3, B_3 and C_3 is point P, then its position is P (x_p, y_p, z_p):

$$\begin{aligned} x_p &= (X_{A_3} + X_{B_3} + X_{C_3})/3 \\ y_p &= (Y_{A_3} + Y_{B_3} + Y_{C_3})/3 \\ z_p &= (Z_{A_3} + Z_{B_3} + Z_{C_3})/3 \end{aligned} \tag{24}$$

By substituting the results of "Eqs. (7)– (9)" in the above equations, the number of direct kinematics position of platform leads to eight solutions which are shown in "Table 2". The comparison of these solutions and the results reported by Shen and et al. [25] show that there is an excellent agreement between these two.

Table 2 Eight solutions for direct kinematics problem of 3-RCC

	x_p	y_p	z_p
1	27.6333	27.6341	-2.3662
2	34.2703	27.6336	-2.3667
3	29.8459	12.0580	22.0585
4	27.6328	4.2707	-2.3662
5	27.6335	4.2703	34.2705
6	27.6336	27.6341	34.2699
7	34.2698	27.6332	34.2705
8	34.2707	4.2708	34.2702

5 CONCLUSION

In this paper, the homotopy continuation method is applied to the direct kinematic problem of the 3RCC Parallel Manipulator. The results reveal that the direct kinematic problem leads to a system of nonlinear equations by 9 equations and 9 unknown parameters for which there are 36 solutions. Finally, the number of direct kinematics position of the 3RCC parallel manipulator is calculated to be 8. The homotopy continuation method proposes some advantages over the conventional methods, including higher convergence speed, while the algorithm is straightforward. Moreover, the algorithm reaches correct values, even if the initial guesses are carelessly chosen. This behavior is interesting since the reputable Newton–Raphson method simply diverges for the same initial guesses. Furthermore, it is shown that the method extracts all possible roots of the system of the nonlinear equations.

6 APPENDIX: AUXILIARY HOMOTOPY FUNCTIONS AND THEIR RESULTS

Functions		Result	
G_1	$-s_{11}$	s_{11}	-32.3668
G_2	$-s_{21}$	s_{21}	-62.3662
G_3	$-s_{31}$	s_{31}	-92.3664
G_4	$-2s_{12}$	s_{12}	23.3627
G_5	s_{22}	s_{22}	36.6360
G_6	s_{32}	s_{32}	6.6377
G_7	$cos\theta_{11}$	θ_{11}	0
G_8	$cos\theta_{21}$	θ_{21}	-1.5708
G_9	$cos\theta_{31}+1$	θ_{31}	-3.1416

Solution No. 1

Functions		Result	
G_1	$2s_{11}$	s_{11}	-32.3658
G_2	$-s_{21}$	s_{21}	-62.3654
G_3	$-s_{31}$	s_{31}	-92.3664
G_4	$-2s_{12}$	s_{12}	23.3634
G_5	$s_{22}-1$	s_{22}	-36.6360
G_6	s_{32}	s_{32}	6.6368
G_7	$tan\theta_{11}$	θ_{11}	0
G_8	$cos\theta_{21}+1$	θ_{21}	133.5177
G_9	$tan\theta_{31}-1$	θ_{31}	-15.7080

Solution No. 2

Functions		Result	
G_1	$-s_{11}$	s_{11}	-32.3668
G_2	$-s_{21}$	s_{21}	-62.3667
G_3	$-s_{31}-2$	s_{31}	-92.3664
G_4	$-2s_{12}$	s_{12}	23.3634
G_5	$-s_{22}-1$	s_{22}	36.6360
G_6	$-s_{32}-1$	s_{32}	-6.6377
G_7	$tan\theta_{11}-1$	θ_{11}	-351.8584
G_8	$sin\theta_{21}+1$	θ_{21}	-1.5708
G_9	$tan\theta_{31}$	θ_{31}	0

Solution No. 3

Functions		Result	
G_1	$-s_{11}-1$	s_{11}	-32.3668
G_2	$s_{21}-2$	s_{21}	-62.3674
G_3	$-s_{31}-1$	s_{31}	-92.3664
G_4	$2s_{12}$	s_{12}	-23.3627
G_5	$s_{22}-1$	s_{22}	36.6360
G_6	$s_{32}-2$	s_{32}	6.6377
G_7	$cos\theta_{11}+3$	θ_{11}	-298.4513
G_8	$sin\theta_{21}+1$	θ_{21}	-7.8540
G_9	$tan\theta_{31}-1$	θ_{31}	442.9646

Solution No. 4

Functions		Result	
G_1	$s_{11}-1$	s_{11}	-32.3661
G_2	$-s_{21}+2$	s_{21}	-62.3667
G_3	$s_{31}+1$	s_{31}	-92.3664
G_4	$2s_{12}$	s_{12}	-23.3634
G_5	$s_{22}-1$	s_{22}	-36.6379
G_6	$s_{32}-2$	s_{32}	6.6371
G_7	$cos\theta_{11}-3$	θ_{11}	47.1239
G_8	$sin\theta_{21}-1$	θ_{21}	1.5708
G_9	$tan\theta_{31}-1$	θ_{31}	-9.4248

Solution No. 5

Functions		Result	
G_1	s_{11}	s_{11}	-32.3661
G_2	$-s_{21}-2$	s_{21}	-62.3662
G_3	$-s_{31}$	s_{31}	-92.3665
G_4	$-2s_{12}+1$	s_{12}	-23.3627
G_5	s_{22}	s_{22}	36.6360
G_6	s_{32}	s_{32}	-6.6362
G_7	$tan\theta_{11}+1$	θ_{11}	15.7080
G_8	$cos\theta_{21}$	θ_{21}	-70.6858
G_9	$tan\theta_{31}$	θ_{31}	0

Solution No. 6

Functions		Result	
G_1	s_{11}	s_{11}	-32.3668
G_2	$-s_{21}$	s_{21}	-62.3655
G_3	s_{31}	s_{31}	-92.3665
G_4	s_{12}	s_{12}	23.3634
G_5	s_{22}	s_{22}	-36.6379
G_6	s_{32}	s_{32}	-6.6370
G_7	$sin\theta_{11}$	θ_{11}	0
G_8	$sin\theta_{21}-1$	θ_{21}	1.5708
G_9	$sin\theta_{31}$	θ_{31}	0

Solution No. 7

Functions		Result	
G_1	$-s_{11}$	s_{11}	-32.3668
G_2	$-s_{21}$	s_{21}	-62.3655
G_3	$-s_{31}$	s_{31}	-92.3665
G_4	$-2s_{12}$	s_{12}	-23.3634
G_5	s_{22}	s_{22}	-36.6360
G_6	s_{32}	s_{32}	-6.6368
G_7	$cos\theta_{11}+1$	θ_{11}	40.8407
G_8	$cos\theta_{21}+1$	θ_{21}	-92.6770
G_9	$cos\theta_{31}+1$	θ_{31}	-12.5664

Solution No. 8

Functions		Result	
G_1	$-s_{11}$	s_{11}	-25.7297
G_2	$-s_{21}$	s_{21}	-62.3662
G_3	s_{31}	s_{31}	-92.3664
G_4	s_{12}	s_{12}	23.3627
G_5	s_{22}	s_{22}	37.2341
G_6	s_{32}	s_{32}	0
G_7	$sin\theta_{11}$	θ_{11}	0
G_8	$sin\theta_{21}$	θ_{21}	-1.3916
G_9	$sin\theta_{31}$	θ_{31}	0

Solution No. 9

Functions		Result	
G_1	$-s_{11}$	s_{11}	-25.7297
G_2	$s_{21}-1$	s_{21}	-62.3667
G_3	$s_{31}-1$	s_{31}	-92.3664
G_4	$2s_{12}-1$	s_{12}	-23.3634
G_5	s_{22}	s_{22}	-37.2341
G_6	s_{32}	s_{32}	0
G_7	$tan\theta_{11}-1$	θ_{11}	12.5664
G_8	$cos\theta_{21}-1$	θ_{21}	-23.3827
G_9	$tan\theta_{31}+1$	θ_{31}	2.9497

Solution No. 10

Functions		Result	
G_1	s_{11}	s_{11}	-25.7297
G_2	s_{21}	s_{21}	-62.3667
G_3	s_{31}	s_{31}	-92.3664
G_4	$-s_{12}$	s_{12}	-23.3634
G_5	$-s_{22}$	s_{22}	37.2339
G_6	$-s_{32}$	s_{32}	0
G_7	$cos\theta_{11}+1$	θ_{11}	-3.1416
G_8	$sin\theta_{21}-1$	θ_{21}	-1.3916
G_9	$cos\theta_{31}+1$	θ_{31}	-0.2739

Solution No. 11

Functions		Result	
G_1	$-s_{11}$	s_{11}	-25.7297
G_2	$-s_{21}$	s_{21}	-62.3667
G_3	s_{31}	s_{31}	-92.3664
G_4	s_{12}	s_{12}	-23.3634
G_5	s_{22}	s_{22}	-37.2341
G_6	s_{32}	s_{32}	0
G_7	$sin\theta_{11}$	θ_{11}	0
G_8	$sin\theta_{21}$	θ_{21}	-1.3916
G_9	$sin\theta_{31}$	θ_{31}	0

Solution No. 12

Functions		Result	
G_1	$-s_{11}$	s_{11}	-32.3668
G_2	$-s_{21}$	s_{21}	-85.7286
G_3	$-s_{31}$	s_{31}	-92.3662
G_4	$-2s_{12}$	s_{12}	0
G_5	s_{22}	s_{22}	36.6360
G_6	s_{32}	s_{32}	24.2872
G_7	$sin\theta_{11}$	θ_{11}	0
G_8	$cos\theta_{21}$	θ_{21}	-1.5708
G_9	$cos\theta_{31}$	θ_{31}	17.0020

Solution No. 13

Functions		Result	
G_1	$-s_{11}$	s_{11}	-32.3668
G_2	$-s_{21}$	s_{21}	-85.7286
G_3	$-s_{31}$	s_{31}	-92.3662
G_4	$-2s_{12}$	s_{12}	0
G_5	s_{22}	s_{22}	-36.6360
G_6	s_{32}	s_{32}	24.2879
G_7	$sin\theta_{11}$	θ_{11}	0
G_8	$sin\theta_{21}$	θ_{21}	83.2522
G_9	$cos\theta_{31}$	θ_{31}	-1.8476

Solution No. 14

Functions		Result	
G_1	$-s_{11}$	s_{11}	-32.3668
G_2	$-s_{21}$	s_{21}	-85.7286
G_3	$-s_{31}$	s_{31}	-92.3667
G_4	$-2s_{12}$	s_{12}	0
G_5	$s_{22}+1$	s_{22}	36.6360
G_6	s_{32}	s_{32}	-24.2872
G_7	$tan\theta_{11}$	θ_{11}	0
G_8	$cos\theta_{21}+1$	θ_{21}	-629.8893
G_9	$tan\theta_{31}-1$	θ_{31}	1.2940

Solution No. 15

Functions		Result	
G_1	$-s_{11}$	s_{11}	-32.3668
G_2	$-s_{21}$	s_{21}	-85.7286
G_3	$-s_{31}$	s_{31}	-92.3667
G_4	$-2s_{12}$	s_{12}	0
G_5	$s_{22}-2$	s_{22}	-36.6360
G_6	s_{32}	s_{32}	-24.2879
G_7	$tan\theta_{11}$	θ_{11}	0
G_8	$cos\theta_{21}+1$	θ_{21}	-17.2788
G_9	$tan\theta_{31}-1$	θ_{31}	1.2940

Solution No. 16

Functions		Result	
G_1	$-s_{11}-1$	s_{11}	-32.3668
G_2	$-s_{21}+2$	s_{21}	-85.7286
G_3	$-s_{31}+1$	s_{31}	-55.7298
G_4	$2s_{12}$	s_{12}	36.6364
G_5	$s_{22}-1$	s_{22}	0
G_6	$s_{32}-2$	s_{32}	24.2874
G_7	$cos\theta_{11}-3$	θ_{11}	447.6770
G_8	$sin\theta_{21}-1$	θ_{21}	1.5708
G_9	$tan\theta_{31}-1$	θ_{31}	-165.2104

Solution No. 17

Functions		Result	
G_1	$-s_{11}-2$	s_{11}	-32.3667
G_2	$s_{21}+1$	s_{21}	-85.7303
G_3	$-s_{31}+1$	s_{31}	-55.7298
G_4	$-2s_{12}$	s_{12}	36.6364
G_5	$-s_{22}-1$	s_{22}	0
G_6	$-s_{32}-2$	s_{32}	-24.2878
G_7	$tan\theta_{11}+3$	θ_{11}	39.2699
G_8	$sin\theta_{21}+1$	θ_{21}	29.8451
G_9	$tan\theta_{31}+1$	θ_{31}	-11.2724

Solution No. 18

Functions		Result	
G_1	s_{11}	s_{11}	-32.3661
G_2	s_{21}	s_{21}	-85.7303
G_3	s_{31}	s_{31}	-55.7292
G_4	$-s_{12}$	s_{12}	-36.6375
G_5	$-s_{22}$	s_{22}	0
G_6	$-s_{32}$	s_{32}	24.2873
G_7	$cos\theta_{11}-1$	θ_{11}	-1.5708
G_8	$sin\theta_{21}-1$	θ_{21}	-1.5708
G_9	$cos\theta_{31}-1$	θ_{31}	-1.8476

Solution No. 19

Functions		Result	
G_1	$-s_{11}$	s_{11}	-32.3668
G_2	$s_{21}+1$	s_{21}	-85.7303
G_3	$-s_{31}+1$	s_{31}	-55.7298
G_4	$-2s_{12}$	s_{12}	-36.6364
G_5	$-s_{22}-1$	s_{22}	0
G_6	$-s_{32}-2$	s_{32}	-24.2874
G_7	$cos\theta_{11}+3$	θ_{11}	-64.4026
G_8	$sin\theta_{21}+1$	θ_{21}	-7.8540
G_9	$tan\theta_{31}+1$	θ_{31}	-42.6883

Solution No. 20

Functions		Result	
G_1	$-s_{11}-1$	s_{11}	-32.3668
G_2	$s_{21}-2$	s_{21}	-62.3671
G_3	$-s_{31}+1$	s_{31}	-55.7300
G_4	$-2s_{12}$	s_{12}	43.4518
G_5	$s_{22}-1$	s_{22}	0
G_6	$s_{32}-2$	s_{32}	6.6364
G_7	$cos\theta_{11}+3$	θ_{11}	-281.7402
G_8	$sin\theta_{21}+1$	θ_{21}	-1.5708
G_9	$tan\theta_{31}-3$	θ_{31}	185.3540

Solution No. 21

Functions		Result	
G_1	$-s_{11}-1$	s_{11}	-32.3668
G_2	$s_{21}-2$	s_{21}	-62.3671
G_3	$-s_{31}+1$	s_{31}	-55.7300
G_4	$2s_{12}$	s_{12}	-43.4518
G_5	$s_{22}-1$	s_{22}	0
G_6	$s_{32}-2$	s_{32}	6.6381
G_7	$cos\theta_{11}+3$	θ_{11}	-303.7314
G_8	$sin\theta_{21}-1$	θ_{21}	133.5177
G_9	$tan\theta_{31}-1$	θ_{31}	235.6194

Solution No. 22

Functions		Result	
G_1	s_{11}	s_{11}	-32.3661
G_2	$-s_{21}-2$	s_{21}	-62.3658
G_3	$-s_{31}$	s_{31}	-55.7301
G_4	$-2s_{12}+1$	s_{12}	43.4518
G_5	s_{22}	s_{22}	0
G_6	s_{32}	s_{32}	-6.6375
G_7	$tan\theta_{11}+1$	θ_{11}	13.5695
G_8	$cos\theta_{21}+1$	θ_{21}	39.9467
G_9	$tan\theta_{31}$	θ_{31}	0

Solution No. 23

Functions		Result	
G_1	$-s_{11}$	s_{11}	-32.3668
G_2	$-s_{21}$	s_{21}	-62.3658
G_3	$-s_{31}$	s_{31}	-55.7301
G_4	$-2s_{12}$	s_{12}	-43.4518
G_5	s_{22}	s_{22}	0
G_6	s_{32}	s_{32}	-6.6364
G_7	$cos\theta_{11}$	θ_{11}	-2.1385
G_8	$cos\theta_{21}$	θ_{21}	-1.5708
G_9	$cos\theta_{31}-1$	θ_{31}	0

Solution No. 24

Functions		Result	
G_1	s_{11}	s_{11}	-25.7286
G_2	$-s_{21}-1$	s_{21}	-62.3659
G_3	$-s_{31}$	s_{31}	-55.7300
G_4	$-2s_{12}+1$	s_{12}	43.4517
G_5	s_{22}	s_{22}	6.6376
G_6	s_{32}	s_{32}	0
G_7	$tan\theta_{11}+1$	θ_{11}	-80.6783
G_8	$cos\theta_{21}+1$	θ_{21}	-508.9380
G_9	$tan\theta_{31}-1$	θ_{31}	-78.7039

Solution No. 25

Functions		Result	
G_1	s_{11}	s_{11}	-25.7304
G_2	$-s_{21}$	s_{21}	-62.3659
G_3	$-s_{31}$	s_{31}	-55.7300
G_4	$-2s_{12}$	s_{12}	-43.4517
G_5	s_{22}	s_{22}	6.6358
G_6	s_{32}	s_{32}	0
G_7	$tan\theta_{11}-1$	θ_{11}	-8.4217
G_8	$cos\theta_{21}-1$	θ_{21}	559.2035
G_9	$tan\theta_{31}+1$	θ_{31}	24.3473

Solution No. 26

Functions		Result	
G_1	$-s_{11}$	s_{11}	-25.7299
G_2	$s_{21}-1$	s_{21}	-62.3670
G_3	$s_{31}-1$	s_{31}	-55.7890
G_4	$-s_{12}-1$	s_{12}	43.4258
G_5	s_{22}	s_{22}	-6.6368
G_6	s_{32}	s_{32}	0
G_7	$tan\theta_{11}+1$	θ_{11}	1.0031
G_8	$cos\theta_{21}-1$	θ_{21}	116.2389
G_9	$tan\theta_{31}+1$	θ_{31}	53.2833

Solution No. 27

Functions		Result	
G_1	s_{11}	s_{11}	-25.7304
G_2	$-s_{21}$	s_{21}	-62.3658
G_3	$-s_{31}$	s_{31}	-55.7300
G_4	$-2s_{12}$	s_{12}	-43.4518
G_5	s_{22}	s_{22}	-6.6358
G_6	s_{32}	s_{32}	0
G_7	$tan\theta_{11}+1$	θ_{11}	-14.7048
G_8	$cos\theta_{21}+1$	θ_{21}	-53.4071
G_9	$tan\theta_{31}-1$	θ_{31}	-65.1880

Solution No. 28

Functions		Result	
G_1	s_{11}	s_{11}	-25.7291
G_2	$-s_{21}$	s_{21}	-85.7286
G_3	$-s_{31}$	s_{31}	-55.7298
G_4	$-s_{12}$	s_{12}	36.6364
G_5	s_{22}	s_{22}	6.6371
G_6	s_{32}	s_{32}	23.3630
G_7	$sin\theta_{11}-1$	θ_{11}	1.5708
G_8	$cos\theta_{21}-1$	θ_{21}	0
G_9	$-sin\theta_{31}+1$	θ_{31}	-1.5708

Solution No. 29

Functions		Result	
G_1	s_{11}	s_{11}	-25.7299
G_2	$-s_{21}$	s_{21}	-85.7286
G_3	$-s_{31}$	s_{31}	-55.7298
G_4	$-s_{12}$	s_{12}	-36.6364
G_5	s_{22}	s_{22}	6.6363
G_6	s_{32}	s_{32}	23.3630
G_7	$sin\theta_{11}+1$	θ_{11}	-1.5708
G_8	$cos\theta_{21}-1$	θ_{21}	0
G_9	$-sin\theta_{31}-1$	θ_{31}	-1.5708

Solution No. 30

Functions		Result	
G_1	s_{11}	s_{11}	-25.7291
G_2	$-s_{21}$	s_{21}	-85.7286
G_3	$-s_{31}$	s_{31}	-55.7298
G_4	$-s_{12}$	s_{12}	36.6364
G_5	s_{22}	s_{22}	-6.6371
G_6	s_{32}	s_{32}	23.3631
G_7	$sin\theta_{11}-1$	θ_{11}	1.5708
G_8	$cos\theta_{21}+1$	θ_{21}	-3.1416
G_9	$-sin\theta_{31}-1$	θ_{31}	-1.5708

Solution No. 31

Functions		Result	
G_1	s_{11}	s_{11}	-25.7291
G_2	$-s_{21}$	s_{21}	-85.7286
G_3	$-s_{31}$	s_{31}	-55.7303
G_4	$-s_{12}$	s_{12}	36.6364
G_5	s_{22}	s_{22}	6.6371
G_6	s_{32}	s_{32}	-23.3630
G_7	$sin\theta_{11}-1$	θ_{11}	1.5708
G_8	$cos\theta_{21}-1$	θ_{21}	0
G_9	$-sin\theta_{31}+1$	θ_{31}	1.5708

Solution No. 32

Functions		**Result**	
G_1	s_{11}	s_{11}	-25.7291
G_2	$-s_{21}$	s_{21}	-85.7286
G_3	$-s_{31}$	s_{31}	-55.7303
G_4	$-s_{12}$	s_{12}	36.6364
G_5	s_{22}	s_{22}	-6.6371
G_6	s_{32}	s_{32}	-23.3631
G_7	$sin\theta_{11} - 1$	θ_{11}	1.5708
G_8	$cos\theta_{21} + 1$	θ_{21}	-3.1416
G_9	$-sin\theta_{31} + 1$	θ_{31}	1.5708

Solution No. 33

Functions		**Result**	
G_1	s_{11}	s_{11}	-25.7291
G_2	$-s_{21}$	s_{21}	-85.7286
G_3	$-s_{31}$	s_{31}	-55.7298
G_4	$-s_{12}$	s_{12}	-36.6364
G_5	s_{22}	s_{22}	-6.6363
G_6	s_{32}	s_{32}	23.3631
G_7	$tan\theta_{11} + 1$	θ_{11}	-1.5708
G_8	$cos\theta_{21} + 1$	θ_{21}	-3.1416
G_9	$-sin\theta_{31} - 1$	θ_{31}	-1.5708

Solution No. 34

Functions		**Result**	
G_1	s_{11}	s_{11}	-25.7299
G_2	$-s_{21}$	s_{21}	-85.7286
G_3	$-s_{31}$	s_{31}	-55.7303
G_4	$2s_{12}$	s_{12}	-36.6364
G_5	s_{22}	s_{22}	6.6363
G_6	s_{32}	s_{32}	-23.3630
G_7	$sin\theta_{11} + 1$	θ_{11}	-1.5708
G_8	$cos\theta_{21} - 1$	θ_{21}	0
G_9	$-sin\theta_{31} + 1$	θ_{31}	1.5708

Solution No. 35

Functions		**Result**	
G_1	s_{11}	s_{11}	-25.7299
G_2	$-s_{21}$	s_{21}	-85.7286
G_3	$-s_{31}$	s_{31}	-55.7303
G_4	$-s_{12}$	s_{12}	-36.6364
G_5	s_{22}	s_{22}	-6.6363
G_6	s_{32}	s_{32}	-23.3631
G_7	$sin\theta_{11} + 1$	θ_{11}	-1.5708
G_8	$cos\theta_{21} + 1$	θ_{21}	-3.1416
G_9	$-sin\theta_{31} + 1$	θ_{31}	1.5708

Solution No. 36

REFERENCES

[1] Gough, V. E., Whitehall, S. G., Universal Tire Test Machine, in: Proceedings of 9th International Technical Congress, F.I.S.I.T.A., Vol. 177, 1962.

[2] Stewart, D. A., Platform with Six Degrees of Freedom, in: Proceedings of the Institute of Mechanical Engineering, Vol. 180, No. 5, 1965, pp. 371–386.

[3] Hunt, K. H., Kinematic Geometry of Mechanism, Clarendon Press, Oxford, 1978.

[4] Fichter, E. F., A Stewart Platform-Based Manipulator: General Theory and Practical Construction, International Journal of Robotics Research, Vol. 5, No. 2, 1986, pp. 157–182.

[5] Mohammadi Daniali, H. R., Zsombor Murray, P. J., and Angeles, J., Singularity Analysis of Planar Parallel Manipulators, Mechanism and Machine Theory, Vol. 30, No. 5, 1995, pp. 665–678.

[6] Merlet, J. P., Gosselin, C. M., and Mouly, N., Workspaces of Planar Parallel Manipulators, Mechanism and Machine Theory, Vol. 33, No. 1–2, 1998, pp. 7–20.

[7] Tsai, M. S., Shiau, T. N., Tsai, Y. J., and Chang, T. H., Direct Kinematic Analysis of a 3-PRS Parallel Mechanism, Mechanism and Machine Theory, Vol. 38, No. 1, 2003, pp. 71–83.

[8] Korayem, M. H., Bamdad, M., Dynamic Load- Carrying Capacity of Cable- Suspended Parallel Manipulators, International Journal of Advance Design and Manufacturing Technology, Vol. 44, 2008, pp. 829–840.

[9] Varedi Koulaei, S. M., Daniali, H. M., Farajtabar, M., Fathi, B., and Shafiee Ashtiani, M., Reducing the Undesirable Effects of Joints Clearance on the Behavior of the Planar 3-RRR Parallel Manipulators, Nonlinear Dynamics, Vol. 86, 2016, pp. 1007–1022.

[10] Shahabi, E., Hosseini, M. A., Kinematic Synthesis of a Novel Parallel Cable Robot as the Artificial Leg, International Journal of Advance Design and Manufacturing Technology, Vol. 9, No. 3, 2016, pp. 1-10.

[11] Varedi, S. M., Daniali, H. M., and Dardel, M., Dynamic Synthesis of a Planar Slider-Crank Mechanism with Clearances, Nonlinear Dynamics, Vol. 79, 2015, pp. 1587–1600.

[12] Dasgupta, B., Mruthyunjaya, T. S., The Stewart Platform Manipulator: a Review, Mechanism and Machine Theory, 35, 2000, pp. 15–40.

[13] Bonev, I. A., Ryu, J., A New Method for Solving the Direct Kinematics of General 6-6 Stewart Platforms, Mechanism and Machine Theory, Vol. 35, 2000, pp. 423–436.

[14] Kachapi, S. H. A., Ganji, D. D., Davodi, A. G., and Varedi, S. M., Periodic Solution for Strongly Nonlinear Vibration Systems by He's Variational Iteration Method, Mathematical Methods in the Applied Sciences, Vol. 32, No. 18, 2009, pp. 2339-2349.

[15] He, J. H., Variational Iteration Method–a Kind of Non-Linear Analytical Technique: Some Examples, International journal of Non-Linear Mechanics, Vol. 34, 1999, pp. 699–708.

[16] He, J. H., A Coupling Method of a Homotopy Technique and a Perturbation Technique for Non-Linear Problems,

International Journal of Non-Linear Mechanics, Vol. 35, 2000, pp. 37–43.

[17] Wu, T. M., A Study of Convergence on the Newton-Homotopy Continuation Method, Applied Mathematics and Computation, Vol. 168, 2005, pp. 1169–1174.

[18] Wu, T. M., The Inverse Kinematics Problem of Spatial 4P3R Robot Manipulator by the Homotopy Continuation Method with an Adjustable Auxiliary Homotopy Function, Nonlinear Analysis, Vol. 64, 2006, pp. 2373–2380.

[19] Morgan, A. P., Wampler, C. W., Solving a Planar Four-Bar Design Problem Using Continuation, ASME Journal of Mechanism Design, Vol. 112, 1990, pp. 544 –550.

[20] Garcia, C. B., Zangwill, W. I., Pathways to Solutions, Fixed Points, and Equilibria, Prentice-Hall Book Company, Inc., Englewood Cliffs, New Jersey, 1981.

[21] Allgower, E. L., Georg, K., Numerical Continuation Methods, An Introduction, Springer, NewYork, 1990.

[22] Varedi, S. M., Daniali, H. M., and Ganji, D. D., Kinematics of an Offset 3-UPU Translational Parallel Manipulator by the Homotopy Continuation Method, Nonlinear Analysis: Real World Applications, Vol. 10, 2009, pp.1767–1774.

[23] Tari, H., Su, H. J., and Li, T. Y., A Constrained Homotopy Technique for Excluding Unwanted Solutions from Polynomial Equations Arising in Kinematics Problems, Mechanism and Machine Theory, Vol. 45, No. 6, 2010, pp. 898–910.

[24] Tari, H., Su, H. J., A Complex Solution Framework for the Kinetostatic Synthesis of a Compliant Four-Bar Mechanism, Mechanism and Machine Theory, Vol. 46, No. 8, 2011, pp. 1137–1152.

[25] Shen, H., Yang, T., Tao, S., Liu, A., and Ma, L. Z., Structure and Displacement Analysis of a Novel Three-Translation Parallel Mechanism, Mechanism and Machine Theory, Vol. 40, 2005, pp. 1181–1194.